

THE EVOLUTION OF CIRCUMSTELLAR PROTOPLANETARY DISCS IN BINARY STAR SYSTEMS

Jeremy L. Smallwood¹, ¹Center for Astrophysics, Space Physics, and Engineering Research, Baylor University, Waco, Texas 76798-7316, USA

Introduction: The majority of stars born in dense stellar clusters are part of binary star systems [5]. Circumbinary discs of gas and dust commonly surround binary star systems and are responsible for accreting material on to the binary [e.g., 1]. The dynamics of the gas flow from the circumbinary disc onto the binary components has significant implications for planet formation scenarios in binary systems.

Circumbinary discs are commonly observed to be moderately to highly misaligned to the binary orbital plane during all phases of stellar evolution. For example, the pre-main sequence binary KH 15D has a circumbinary disc inclined by $3 - 15^\circ$ [4, 19]. The radial extent of the disc is narrow and presumed to be rigidly precessing in order to explain the unique periodic light curve. Another pre-main-sequence binary, GG Tau A, was observed to contain a circumbinary disc tilted by about 37° [10]. A $\sim 60^\circ$ inclined circumbinary disc is found around the main-sequence binary IRS 43 [3], along with misaligned circumstellar discs around each binary component. There is an observed misalignment of about 70° between the circumbinary disc and the circumprimary disc in HD 142527 [13]. Another main-sequence binary, HD98800BaBb, has the only observed polar (inclined by $\sim 90^\circ$) gaseous circumbinary disc [9]. The 6–10 Gyr old binary system, 99 Herculis, has a nearly polar (about 87°) debris ring [8, 20].

A misaligned disc undergoes nodal precession and evolves towards either a coplanar or polar alignment due to viscous dissipation [2, 11, 12, 14]. Misaligned discs around an eccentric binary undergo tilt oscillations as they align due to the asymmetric potential produced by the eccentric binary [19, 20].

A misaligned circumbinary disc may form misaligned circumstellar discs around the individual binary components [e.g., 17, 21]. A highly misaligned disc around one component of a binary undergoes KL cycles where the inclination is exchanged for eccentricity [15]. Due to the disc viscosity, these oscillations are damped. KL oscillations can occur in a fluid disc with a wide variety of disc and binary parameters. When the disc becomes eccentric, it overflows its Roche lobe and transfers material to the companion star [6]. Self-gravity of a disc can suppress disc KL oscillations if the disc is close to being gravitationally unstable. KL oscillations in a circumstellar disc may have significant consequences for planet formation since strong shocks in the gas are produced during high eccentricity phases [7].

In this work, we first simulate the flow of material

originating from a misaligned circumbinary disc to track the formation and evolution of circumstellar discs around each binary component.

Methods: We use the smoothed particle hydrodynamics (SPH) code PHANTOM [18] to model gaseous circumbinary and circumstellar discs. PHANTOM has been tested extensively for modeling misaligned circumbinary discs [16, 19]. We model the binary star system as a pair of sink particles, with an initial binary separation a . Each sink particle is given an initial mass with M_1 being the primary mass and M_2 being the secondary mass. The simulations assume an equal-mass binary ($M_1 = M_2$). In Cartesian coordinates, the orbit of the binary lies in the x - y plane initially. The binary begins initially at apastron along the x -axis. A large accretion radius is often used to reduce the computation time significantly by neglecting to resolve close-in particle orbits. Since we are interested in resolving the formation and evolution of the circumstellar material, we adopt a relatively small accretion radius of $0.05a$.

To model an initially flat but tilted gaseous circumbinary disc, we follow the methods of [21]. The disc initially consists of 1.5×10^6 equal-mass Lagrangian SPH particles. The simulations are run for $45 P_{\text{orb}}$, where P_{orb} is the orbital period of the binary. This is sufficient time for the forming circumstellar discs to reach a quasi-steady state. We simulate various initial circumbinary disc inclinations of $i_0 = 0^\circ, 20^\circ, 40^\circ, 60^\circ, 90^\circ$. A disc with $i_0 = 0^\circ$ is coplanar to the binary orbital plane and a disc with $i_0 = 90^\circ$ is in a polar configuration. All of the simulations model a low-mass circumbinary disc such that $M_{\text{CBD}} = 10^{-3}M$, where M is the total binary mass ($M = M_1 + M_2$).

Results: To analyze the data on the circumbinary disk, we average over all particles which range from the innermost bound circumbinary particle out to a distance of $3a$. For the circumstellar disks, we average over all particles that are bound to each binary component (i.e., the specific energies, kinetic plus potential, of the particles are negative, neglecting the thermal energy). For each disk, we calculate the mean properties of the particles such as the surface density, inclination, longitude of ascending node, and eccentricity.

We examine a circumbinary disc with an initial misalignment of $i_0 = 60^\circ$ and 90° . The top row in Fig. 1 shows the initial circumbinary disc structure for the two misalignments in the x - z plane. The bottom row shows the disc structure at a time of $25 P_{\text{orb}}$. Material flows

from the circumbinary disc, and forms circumstellar discs around each binary component.

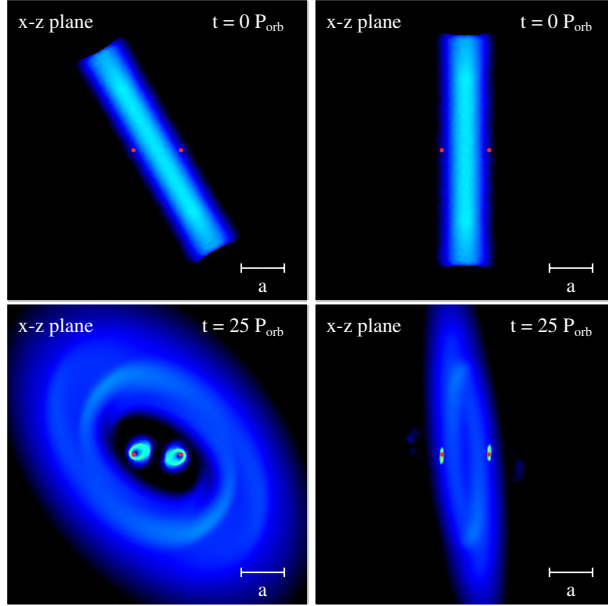


Figure 1: Top row: initial circumbinary disc structure misaligned by 60 and 90°. Bottom row: disc structure at a time of 25 P_{orb} . Circumstellar stellar discs are forming around each binary component (red dots). The color denotes the gas density using a weighted density interpolation. The yellow regions are about three orders of magnitude larger than the blue.

Figure 2 shows the tilt, i and eccentricity, e , of the circumprimary disc for both initial circumbinary disc misalignments. The forming circumstellar discs undergo long-lived KL oscillations from the continuous accretion of material from the circumbinary disc. For the polar simulation, the forming circumstellar discs form with an initial inclination close to polar. The primary disc forms with an eccentricity of ~ 0.25 . The polar circumstellar discs undergo the KL instability, which forces the disc eccentricity and tilt to oscillate in time. The presence of accretion from the circumbinary disc allows the KL instability to operate in the polar regime.

Summary: In this work, we further investigate the flow of material from a circumbinary disc, which aid in the formation of circumstellar discs around each binary component, and the formation of exoplanets. Highly inclined circumstellar discs around individual binary components trigger the KL mechanism. During KL cycles, the disc structure is altered by exchanging disc eccentricity with disc tilt and vice versa. The continuous accretion of material from the circumbinary disc allows the KL cycles to be long-lived. During this process, the circumbinary material is continuously delivered with a high inclination to the lower tilted circum-single disc. Accretion

keeps the tilt of the disc high and allows the KL cycles to continue for a more extended period. An initially polar circumbinary disc forms nearly polar circumstellar discs around each binary component. The continuous accretion of polar circumbinary material onto the polar circumstellar discs causes the KL mechanism to be sustained over many KL oscillation periods. The KL unstable polar circumstellar discs may give rise to the formation of polar S-type planets.

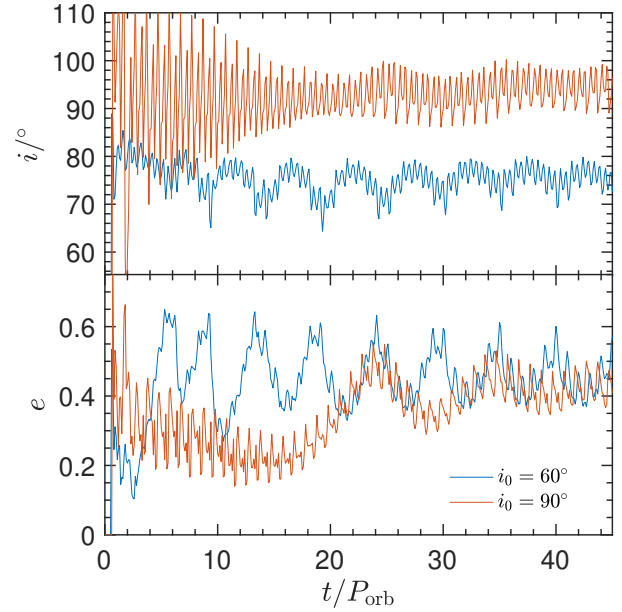


Figure 2: The inclination and eccentricity of the circumprimary disc in the simulations with an initial circumbinary disc tilted by 60° (blue) and 90° (red).

References: [1] Alves F. O. et al. 2019, *Science*, 366, 90. [2] Aly H. et al. 2015, *MNRAS*, 449, 65. [3] Brinch C. et al. 2016, *ApJ*, 830, L16. [4] Chiang E. I. and Murray-Clay R. A., 2004, *ApJ*, 607, 913. [5] Duquennoy A. and Mayor M., 1991, *AA*, 248, 485. [6] Franchini A. et al. 2019, *MNRAS*, 485, 315. [7] Fu W. et al., 2017, *ApJ*, 835, L29 [8] Kennedy G. M. et al., 2012, *MNRAS*, 421, 2264. [9] Kennedy G. M. et al., 2019, *Nature Astronomy*, 3, 230. [10] Keppler M. et al., 2020, *AA*, 639, A62. [11] Larwood J. D. et al., 1996, *MNRAS*, 282, 597. [12] Lubow S. H. and Ogilvie G. I., 2000, *ApJ*, 538, 326. [13] Marino S. et al., 2015, *ApJ*, 798, L44. [14] Martin R. G. and Lubow S. H., 2018, *MNRAS*, 479, 1297. [15] Martin R. G. et al., 2014a, *ApJL*, 790, L34. [16] Nixon C. J., 2012, *MNRAS*, 423, 2597. [17] Nixon C. et al., 2013, *MNRAS*, 434, 1946. [18] Price D. J., et al., 2018, *Publ. Astron. Soc. Australia*, 35, e031. [19] Smallwood J. L. et al., 2019, *MNRAS*, 486, 2919 [20] Smallwood J. L. et al., 2020, *MNRAS*, 494, 487. [21] Smallwood J. L. et al., 2021b, *ApJ*, 907, L14.